

# Quantized pumped charge due to surface acoustic waves in a 1D channel

Amnon Aharony and O. Entin-Wohlman

School of Physics and Astronomy, Raymond and Beverly Sackler Faculty of Exact Sciences,  
Tel Aviv University, Tel Aviv 69978, Israel

(November 2, 2018)

The adiabatic pumped current through an unbiased one dimensional (1D) channel, connected to two 1D leads and subject to surface acoustic waves (SAW), is calculated exactly for non-interacting electrons. For a broad range of the parameters, quantum interference generates a staircase structure of the time-averaged current, similar to experimental observations. This corresponds to integer values (in units of electronic charge) of the charge pumped during each period of the SAW. We also find staircases for higher harmonics. Quantum interference can thus replace Coulomb blockade in explaining the pumped charge quantization, particularly in the SAW experiments.

73.23.-b,73.63.Rt,73.50.Rb,73.40.Ei

Mesoscopic devices which exhibit quantized dc currents may serve as accurate current standards, to be used in single-electron metrology. [1] Theoretically, such quantization was first suggested by Thouless, [2] for non-interacting electrons subject to a slowly moving periodic potential which is superimposed on an infinite periodic system. This model is an example of *adiabatic quantum charge pumping*, [3] a phenomenon which attracted much recent theoretical interest. [4–18] In such pumping, an oscillating potential, with period  $\tau = 2\pi/\omega = 1/f$ , generates a time-averaged current  $\bar{I}$  *without any bias between the two terminals*. Under ideal conditions,  $\bar{I}$  has the quantized values  $\mathcal{N}ef$ , with an integer  $\mathcal{N}$ , where  $e$  is the electron charge. This implies that the charge  $Q$  transferred during time  $\tau$  is  $Q = \mathcal{N}e$ . The direction of the current is determined by phase shifts between the oscillating potential at different locations.

Quantized pumped currents have been observed in two types of experiments. In the first, the periodically moving potential is provided by the piezoelectric potential of *surface acoustic waves* (SAW) generated in a quasi-one-dimensional (1D) GaAs-AlGaAs channel, [19,20] and the observed average acoustoelectric current exhibits steps between plateaus at  $\mathcal{N}ef$  as function of either the gate voltage,  $V$ , or the amplitude of the SAW,  $P$ . In the second, out-of-phase oscillatory voltages were applied to the barriers connecting a quantum dot (QD) to the leads, in *turnstile-type devices*. [21–23] In both cases, the apparent quantization of  $Q$  was attributed to the Coulomb blockade which dictates the integral number of electrons ‘carried’ by the moving potential well. Although such explanations may apply to almost closed dots, electron-electron interactions should be less important in *almost open dots* (as used e. g. in [21]).

Adiabatic unbiased quantum pumping for *non-interacting electrons* was recently studied for the turnstile-like geometry. [13] When the Fermi energy in the leads  $E_F$  aligns with the energy of the quasi-bound state in the QD,  $Q/e$  was found to be close to one. Along

similar lines, [14] the existence of resonant states in a QD was found to greatly enhance the magnitude of  $Q$ , causing it to change sharply as function of some parameters. Here we present a simple model for the SAW experiment, which exhibits steps and integer plateaus in  $Q$ , as function of parameters, for *non-interacting electrons*. Each step in  $Q$  is accompanied by a narrow peak in the otherwise very small time-averaged transmission  $\bar{T}$ . The calculated staircase plots (e. g. Fig. 1 below), and the accompanying peaks in  $\bar{T}$ , are qualitatively reminiscent of the quantum Hall transverse and longitudinal resistances. Indeed, both effects follow from steps in Berry-like phases of the quantum wave functions, resulting only from *quantum interference*. [2,4,5] Interestingly, our results are also similar to those observed in the SAW experiments.

Unlike the turnstile-like case, the piezoelectric potential generated by the SAW oscillates with time *everywhere* inside the nanostructure,  $\mathcal{H}_{\text{SAW}}(\mathbf{r}, t) = P \cos(\omega t - \mathbf{q} \cdot \mathbf{r})$ , with the SAW wavevector  $\mathbf{q}$ , while being heavily screened by the 2DEG forming the leads. SAW usually satisfy the adiabatic conditions, as  $\hbar\omega$  is small compared to the relevant electronic energy scales. [2] In the absence of bias, SAW generate a non-zero average current, in the direction of  $\mathbf{q}$ . A realistic treatment of the experimental geometry [12] only allowed a calculation at low  $P$ , yielding  $Q \propto P^2$ . The decay of  $\mathcal{H}_{\text{SAW}}$  in the wide banks of the channel is also difficult to treat exactly. In order to obtain a simple solvable model, we simplify all of these by a 1D tight-binding model. The ‘channel’ is made of sites  $n = 1, 2, \dots, N$ . It is connected to two 1D ‘leads’ via sites 1 and  $N$ . The leads, which connect to electron reservoirs (with the same chemical potential), are described by  $\mathcal{H}_0 = -J \sum_n (|n\rangle\langle n+1| + hc)$  for  $n < 0$  and  $n > N$ , with eigenfunctions like  $e^{\pm ikan}$  and energies  $E = -2J \cos ka$ , where  $a$  is the lattice constant. The ‘channel’ is modeled by

$$\mathcal{H}_{\text{osc}} = \sum_n \{ \epsilon_n(t) |n\rangle\langle n| - J_n (|n\rangle\langle n+1| + hc) \}. \quad (1)$$

with  $J_n = J_D$  inside the channel, i. e. for  $1 \leq n \leq N-1$ ,

and  $J_0 = J_\ell$ ,  $J_N = J_r$  for the ‘contacts’ with the leads. To model  $\mathcal{H}_{\text{SAW}}(\mathbf{r}, t)$ , we choose the site energies inside the channel ( $1 \leq n \leq N$ ) as

$$\epsilon_n(t) = V + P \cos[\omega t - qa(n - n_0)], \quad (2)$$

where  $V$  represents the gate voltage and  $P > 0$ , so that  $\epsilon_n$  has a maximum (or minimum) in the center of the channel  $n_0 = (N + 1)/2$  at  $t = 0$  (or  $\tau/2$ ). This potential acts only inside the channel, imitating the screening of the SAW outside.

Figure 1 shows  $Q$  (in units of  $e$ ) versus  $V$  for  $N = 6$  and some ‘optimal’ parameters, at zero temperature ( $T = 0$ ). One clearly observes three plateaus at each end, with  $Q/e$  very close to  $\pm N$  and  $N = 0, 1, 2, 3$ . Generally, we observe sharp plateaus up to  $N/2$ , with possibly several additional rounded peaks or spikes. The steps, at  $V_N$ , between these plateaus appear to be equidistant; for large  $N$  we show below that

$$\begin{aligned} V_N &\approx E_F \pm \left( P + 2J_D - \Delta \left( N + \frac{1}{2} \right) \right), \\ \Delta &= qa\sqrt{2PJ_D}, \end{aligned} \quad (3)$$

i. e. the steps move outwards (left and right) and broaden with increasing  $P$  and  $J_D$ , as also happens qualitatively in the experiments. [19,20] It would be nice to examine this detailed quantitative prediction experimentally. As one expects,  $Q = 0$  when any one of  $P$ ,  $J_L$ ,  $J_D$ ,  $qa$ ,  $ka$  or  $E_F - V$  vanishes. Indeed, the steps become rounded and decrease gradually as  $P$ ,  $E_F - V$  or  $qa$  approach zero. The rounding begins at the larger  $N$ 's; the plateaus at  $N = \pm 1$  disappear last. The results remain robust for a wide range of  $ka$ ,  $J_L$  and  $J_D$ , provided  $0 < J_L^2/J \leq J_D \ll P$ ,  $|E_F - V|$ ; Fig. 2 shows the effects of increasing  $J_D$ , and of going to the limit of a completely open channel ( $J_L = 1$  and  $ka = \pi/2$ ). In the latter case, electron-electron interactions should be unimportant! As Eq. (3) implies, we also observe steps and plateaus for  $Q$  versus  $P$  at fixed  $V$ : at low  $P$ , one starts with  $Q \propto P^2$ , but  $Q$  remains very small up to  $P_0 = E_F - V - 2J_D + \Delta/2$ . Above  $P_0$  one observes  $N/2$  steps, at intervals  $\Delta$  (which now increases with  $P$ ), and then a gradual decrease towards zero. Thus, both  $V$  and  $P$  can be used as triggers for on-off switching of the pumped current.

The ‘optimal’ graph in Fig. 1 was derived at  $qa = \pi/[2(N - 1)]$ , corresponding to a total phase shift of  $\pi/2$  between the end points ( $n = 1$  and  $N$ ), or to a SAW wave length  $\lambda$  equal to  $4L$ , where  $L = (N - 1)a$  is the length of the channel. Figure 3 shows results for  $\lambda/L = 1, 1.5, 2$  and  $8$ ; clearly, the staircase deteriorates as  $\lambda$  moves away from  $4L$ , in both directions. Even as the higher plateaus deteriorate, the plateaus at  $N = \pm 1$  remain quite robust, down to  $\lambda \sim L$  as apparently used in the experiments. [19] Note that in the latter, the SAW decays towards the ends of the channel, and therefore the relevant  $L$  may be

smaller than estimated, bringing the experiments closer to our ‘optimal’ range.

Our calculations involve three main steps. In the first, we use the adiabatic approximation (neglecting high orders in time-derivatives of the wave functions) to calculate the unbiased current. Such calculations usually employ the Brower formula [6], which involves integrals over the multidimensional space of the time-dependent potentials. Here we use an equivalent formula, which is more convenient for a general  $\mathcal{H}_{\text{osc}}$ . If  $|\chi_\alpha^t\rangle$  denotes the instantaneous scattering solution at time  $t$ , which results from an incoming wave  $|w_\alpha^-\rangle$  from lead  $\alpha$  ( $= \ell, r$ ) with energy  $E$ , then the instantaneous current from left to right is [24]

$$I_\ell^t = \frac{e}{2\pi} \int dE \left( -\frac{\partial f}{\partial E} \right) \langle \chi_\ell^t | \dot{\mathcal{H}}_{\text{osc}} | \chi_\ell^t \rangle, \quad (4)$$

where  $f(E)$  is the Fermi distribution (which is the same in both leads, in the unbiased limit), and the dot denotes the time derivative. Below we use  $T = 0$ , i. e.  $E = E_F$ . Using (4), the charge pumped in one period becomes  $Q_\ell = \int_{-\tau/2}^{\tau/2} dt I_\ell^t$ . For a symmetric channel ( $J_\ell = J_r$ ) one has  $Q_\ell = -Q_r = (Q_\ell - Q_r)/2 \equiv Q \equiv \bar{I}\tau$ .

The second step involves finding  $|\chi_\alpha^t\rangle$ . This is similar to a static scattering solution: we write

$$\begin{aligned} \langle n | \chi_\ell^t \rangle &= A_{0,\ell} e^{ikan} + A_\ell e^{-ikan}, \quad n \leq 0, \\ \langle n | \chi_\ell^t \rangle &= B_\ell e^{ikan}, \quad n \geq N + 1, \end{aligned} \quad (5)$$

with  $A_{0,\ell} = 1/\sqrt{2J \sin ka}$  (for a unit incoming flux). The Schrödinger equations at the sites  $n = 0$  and  $n = N + 1$  now yield  $A_{0,\ell} e^{ika} + A_\ell e^{-ika} = \phi_\ell(1) J_\ell/J$  and  $B_\ell e^{ikNa} = \phi_\ell(N) J_r/J$ , where  $\{\phi_\ell(n)\}$  are the amplitudes of the scattering solution inside the nanostructure, which obey

$$\begin{aligned} \sum_{n'} \mathcal{M}_{nn'} \phi_\ell(n') &= 2\delta_{n,1} i \sin ka e^{ika} J_\ell A_{0,\ell}, \\ \mathcal{M}_{n,n'} &\equiv (g^{-1}(E))_{n,n'} = E\delta_{n,n'} - (\mathcal{H}_{\text{osc}})_{n,n'} \\ &+ \delta_{n,n'} e^{ika} (\delta_{n,1} J_\ell^2 + \delta_{n,N} J_r^2)/J, \end{aligned} \quad (6)$$

for  $1 \leq n, n' \leq N$ . The solution of these equations is

$$\begin{aligned} \phi_\ell(n) &= e^{ika} A_{0,\ell} 2i \sin ka J_\ell g_{n,1}, \\ A_\ell &= e^{2ika} A_{0,\ell} [2i \sin ka g_{1,1} J_\ell^2/J - 1], \\ B_\ell &= e^{ika(1-N)} A_{0,\ell} 2i \sin ka g_{N,1} J_\ell J_r/J, \end{aligned} \quad (7)$$

with similar expressions for  $\phi_r(n)$ ,  $A_r$  and  $B_r$ . The last equation in (7) yields the instantaneous (‘normal’) transmission,  $\mathcal{T}^t = 4|g_{N,1}|^2 (J_\ell J_r/J)^2 \sin^2 ka$ . In the cases of interest here,  $\mathcal{T}^t$  is usually very small. However,  $\mathcal{T}^t$  has local peaks (as function of  $\cos \omega t$ ) at the  $N$  poles of  $g_{N,1}$ , i. e. the zeroes of  $D(\cos \omega t) = \det \mathcal{M}$ . The time-average  $\bar{\mathcal{T}} = \int_{-\tau/2}^{\tau/2} dt \mathcal{T}^t / \tau$  thus exhibits peaks wherever such poles occur within the period  $\tau$ .

If  $\mathcal{H}_{\text{osc}}$  depends on time only via  $\epsilon_n$ , then Eq. (4) yields

$$Q_\ell = \frac{eJ_\ell^2 \sin ka}{\pi J} \int_{-\tau/2}^{\tau/2} dt \sum_{n=1}^N \dot{\epsilon}_n |g_{n,1}|^2. \quad (8)$$

and  $Q_\ell$  shows singularities whenever  $\cos \omega t$  comes close to one or more zeroes of  $D$  within the integration. For small  $(J_\ell^2 + J_r^2)/J$ , these poles have small imaginary parts, and  $Q$  exhibits large changes whenever  $\cos \omega t$  passes near such a pole. These steps occur exactly when  $\bar{T}$  has spikes, originating from the same poles.

In the third step, we apply the above adiabatic equations to our specific 1D channel model. The  $N \times N$  matrix  $\mathcal{M} = g^{-1}(E)$  is now tridiagonal, with  $\mathcal{M}_{n,n} = E - \epsilon_n + e^{ika}(\delta_{n,1}J_\ell^2 + \delta_{n,N}J_r^2)/J$  and  $\mathcal{M}_{n,n\pm 1} = J_D$ . Since  $\dot{\epsilon}_n = -\omega P \sin[\omega t - qa(n - n_0)]$ ,  $I_\ell^t$  is equal to  $\omega$  times a function of  $\omega t$ ,  $\bar{I} \propto \omega$  and  $Q$  is independent of  $\omega$ . For our symmetric channel ( $J_\ell = J_r$ ),  $D$  is an order- $N$  polynomial in  $\cos \omega t$ ; we calculate  $Q$  by rewriting the integrand as a sum over its  $2N$  complex poles in  $\cos \omega t$ , and using analytic expressions for  $\int_0^\pi du u^m / (\cos u - z)$ .

It is interesting to follow these poles as function of the various parameters. For this purpose, we show in Fig. 4 the partial charge  $Q_\ell(t)$ , resulting from integration of Eq. (8) only up to  $t < \tau/2$ , at different values of  $V$ . As  $V$  increases through  $V_1$ ,  $Q_\ell(t)$  suddenly exhibits a step from zero to one, which appears at  $t = 0$ . This step corresponds to a pole in  $I_\ell^t$ , which enters near  $\cos \omega t = 1$ . As  $V$  increases, this step moves to the left. At  $V = V_2$ , another step (from 1 to 2) enters at  $t = 0$ . For large  $N$ , the time interval between two consecutive steps is roughly equal to  $\delta = qa/\omega$ . As  $V$  increases further, both steps move to the left, and at  $V = V_3$  a step from 2 to 3 enters at  $t = 0$ . After a narrow intermediate complex state, there begin to enter steps of  $-1$ , until at  $V = E_F$  we observe exactly  $N/2$  steps of  $+1$  followed by  $N/2$  steps of  $-1$ , ending up with  $Q = 0$ . A similar build-up of (negative) steps occurs when one starts at large positive  $V$ , and follows  $V$  down through  $V_{-N}$ , except for the fact that now the new steps show up at  $t = \tau/2$ , i. e.  $\cos \omega t = -1$ . The physical interpretation of these results is clear: unlike the Coulomb blockade picture, where  $\mathcal{N}$  electrons move together from left to right, carried by a single minimum of the moving potential, in the SAW case treated here  $Q_\ell$  changes by steps of 1, implying *separate motion of individual electrons*, building up to  $\mathcal{N}$  after a full period. The picture is particularly interesting near  $V = E_F$ : during a period,  $Q_\ell(t)$  exhibits several positive steps, and then an equal number of negative steps, ending with no net pumped charge.

The step-like time dependence of  $Q_\ell(t)$  immediately implies the appearance of *higher harmonics* (in  $\omega$ ) of the pumped current: for  $V$  in the  $\mathcal{N}$ 'th plateau, we approximate  $I_\ell^t \approx e \sum_{j=1}^{\mathcal{N}} \delta(t - t_j)$ , with  $t_j = t_0(V) + (j - 1)\delta$ . The pumped current then becomes  $I_\ell^t = ef \{ \mathcal{N} + 2 \sum_{m=1}^{\infty} \cos[m\omega(t - t_0 - (\mathcal{N} - 1)\delta/2)] \mathcal{I}(m, \mathcal{N}) \}$ , with

$$\mathcal{I}(m, \mathcal{N}) \approx \sin(\mathcal{N}m\omega\delta/2) / \sin(m\omega\delta/2). \quad (9)$$

Thus, this  $m$ 'th harmonic amplitude also exhibits a staircase structure. Although  $|\mathcal{I}(m, 1)|^2 \equiv 1$ , the plateaus at higher  $\mathcal{N}$  oscillate with  $m$ . It is interesting to note that harmonics with  $m \neq 0$  survive in the intermediate range  $V \sim E_F$ : as seen from the center Fig. 4, one then has a difference like  $\cos[m\omega(t - t_1)] - \cos[m\omega(t - t_2)]$ . It would be very interesting to study  $\mathcal{I}(m, \mathcal{N})$  experimentally.

Since the steps in  $Q(V)$  arise when poles appear (or disappear) when  $\cos \omega t = \pm 1$ , we confirmed that the  $V_{\mathcal{N}}$ 's are the solutions of  $D(V, \cos \omega t = \pm 1) = 0$ . Taking  $t = \tau/2$ , this equation is equivalent to the set of equations

$$(E - V + P \cos[(n - n_0)qa])\phi(n) = -J_D[\phi(n+1) + \phi(n-1)] \quad (10)$$

for  $1 < n < N$ , with modified equations for  $n = 1$  and  $n = N$ . Except for the boundaries, these are Mathieu's equations, with the symmetric potential having a minimum at  $n = n_0$ . This can be written as

$$-J_D[\phi(n+1) + \phi(n-1) - 2\phi(n)] + P(1 - \cos[(n - n_0)qa])\phi(n) = E\phi(n), \quad (11)$$

with  $E = E - V + P + 2J_D$ . For our 'optimal'  $qa = \pi/[2(N - 1)]$ , one has  $|n - n_0|qa \leq \pi/4$ , so that the replacement  $1 - \cos[(n - n_0)qa] \approx \frac{1}{2}(n - n_0)^2(qa)^2$  forms an excellent approximation. The low lying eigenenergies of the isolated channel then correspond to localized states around  $n_0$ , which are not very affected by the boundaries. For large  $N$ , we also use  $[\phi(n+1) + \phi(n-1) - 2\phi(n)] \approx \partial^2 \phi / \partial n^2$ . Eq. (11) then becomes the Schrödinger equation for the harmonic oscillator, yielding the eigenvalues  $E_{\mathcal{N}} = \Delta(\mathcal{N} + 1/2)$ , with integer  $\mathcal{N}$ , i. e. Eq. (3) with the upper sign. The solution for the other sign, associated with poles entering at  $t = 0$ , follows the replacement  $\phi(n) \rightarrow (-1)^n \phi(n)$ . These approximate values agree very well with our direct solutions of  $D(V, \pm 1) = 0$  and with the steps in  $Q$ , even for relatively small  $N$  (e. g. Fig. 1).

A few more comments are in place: (a) Although our calculated plateaus look like constant integers, in practice the function  $Q(V)$  remains slightly below  $\mathcal{N}$ , reaching a smooth maximum around the middle of the 'plateau'. For  $N = 6$ , the difference  $(\mathcal{N} - Q(V))$  is of order .0001. This difference becomes smaller for larger  $N$ . (b) Our robust plateaus at integer values occur only for the model presented here, where the amplitude  $P$  has exactly the same value for all  $n$  in the channel. Modulation of  $P$  in space, e. g. due to a screening decay, due to a reflected SAW, [20] or due to random energies  $\{V_n\}$ , gives plateaus at non-integer values or round the steps. This, and a treatment of more complex nanostructures, will be reported elsewhere. [24] (c) Our formalism allows for  $T > 0$ , where we only expect some rounding of the steps. (d) Eq. (3) for  $\Delta$  remains true in the limit  $N \rightarrow \infty$ ,  $a \rightarrow 0$ ,  $(N - 1)a = L$ ,

when  $J_D a^2 \rightarrow \hbar^2/(2m^*)$ . (e) Finally, we emphasize again that all of our results are valid only in the adiabatic limit.

We thank Y. Imry, Y. Levinson and P. Wölfle for helpful conversations. This research was carried out in a center of excellence supported by the Israel Science Foundation, and was supported in part by the National Science Foundation under Grant No. PHY99-07949 and by the Einstein Center at the Weizmann Institute.

- 
- [1] K. Flensberg *et al.*, Int. J. Mod. Phys. B **13**, 2651 (1999).
  - [2] D. J. Thouless, Phys. Rev. B **27**, 6083 (1983).
  - [3] F. Hekking and Yu. V. Nazarov, Phys. Rev. B **44**, 9110 (1991).
  - [4] B. L. Altshuler and L. I. Glazman, Science **283**, 1864 (1999).
  - [5] G. B. Lubkin, Phys. Today, June 1999, p. 19.
  - [6] P. W. Brouwer, Phys. Rev. B **58**, R10135 (1998).
  - [7] I. L. Aleiner and A. V. Andreev, Phys. Rev. Lett. **81**, 1286 (1998).
  - [8] F. Zhou, B. Spivak, and B. L. Altshuler, Phys. Rev. Lett. **82**, 608 (1999).
  - [9] T. A. Shutenko, I. L. Aleiner and B. L. Altshuler, Phys. Rev. B **61**, 10366 (2000).
  - [10] S. H. Simon, Phys. Rev. B **61**, R16327 (2000).
  - [11] P. A. Maksym, Phys. Rev. B **61**, 4727 (2000).
  - [12] Y. Levinson, O. Entin-Wohlman and P. Wölfle, Phys. Rev. Lett. **85**, 634 (2000).
  - [13] Y. Levinson, O. Entin-Wohlman, and P. Wölfle, cond-mat/0010494 (2000).
  - [14] Y. Wei, J. Wang, and H. Gou, Phys. Rev. B **62**, 9947 (2000).
  - [15] M. Moskalets and M. Büttiker, Phys. Rev. B **64**, 201305 (2001).
  - [16] P. Sharma and C. Chamon, Phys. Rev. Lett. **87**, 096401 (2001).
  - [17] Y. Makhlin and A. Mirlin, cond-mat/0105414 (2001).
  - [18] Y. Wei, J. Wang, H. Guo, and C. Roland, Phys. Rev. B **54**, 115321 (2001).
  - [19] J. M. Shilton, V. I. Talyanskii, M. Pepper, D. A. Ritchie, J. E. F. Frost, C. J. Ford, C. G. Smith and G. A. C. Jones, J. Phys.: Condens. Matter **8**, L531 (1996).
  - [20] V. I. Talyanskii, J. M. Shilton, M. Pepper, C. G. Smith, C. J. Ford, E. H. Linfield, D. A. Ritchie, and G. A. C. Jones, Phys. Rev. B **56**, 15180 (1997).
  - [21] M. Switkes, C. M. Marcus, K. Campman and A. C. Gosard, Science **283**, 1905 (1999).
  - [22] H. Pothier, P. Lafarge, U. Urbina, D. Esteve and M. H. Devoret, Europhys. Lett. **17**, 249 (1992).
  - [23] L. P. Kouwenhoven, A. T. Johnson, N. C. van der Vaart, A. van der Enden, C. J. P. M. Harmans, and C. T. Foxon, Z. Phys. B **85**, 381 (1991).
  - [24] O. Entin-Wohlman, A. Aharony and Y. Levinson, unpublished.

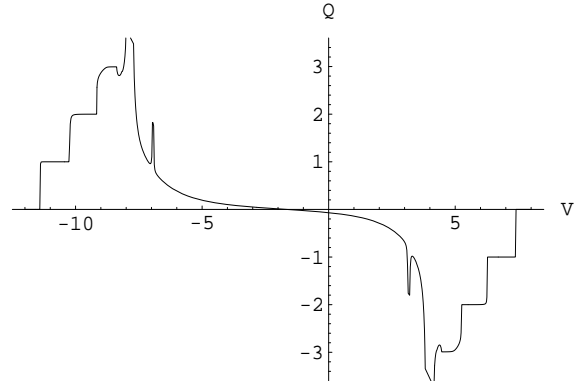


FIG. 1. Pumped charge  $Q$  (in units of  $e$ ) versus the gate voltage  $V$  (in units of  $J$ ) for  $N = 6$ ,  $P = 8J$ ,  $J_D = J$ ,  $J_\ell = J_r = J_L = .4J$ ,  $qa = \pi/10$ ,  $ka = \pi/100$ .

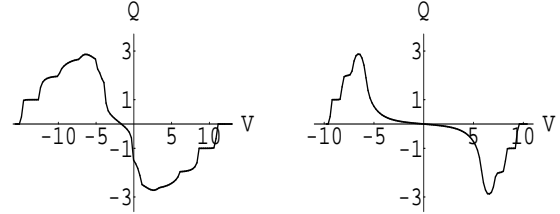


FIG. 2. Same as Fig. 1, but with  $J_D = 3J$  (left) and  $J_L = J$ ,  $ka = \pi/2$  (right).

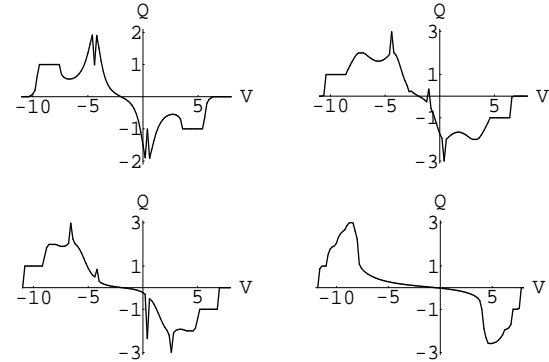


FIG. 3. Same as Fig. 1, but with  $qa = 2\pi/5, 4\pi/15, \pi/5$  and  $\pi/20$ , corresponding to  $\lambda/L = 1, 1.5, 2$  and  $8$ .

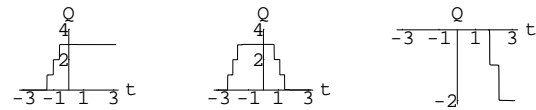


FIG. 4. Partial pumped charges  $Q_\ell$ , in units of  $e$ , up to time  $t$  within a period, for the same parameters as in Fig. 1, with  $V/J = -8.6, -2$  and  $5.3$ . The  $t$ -axis shows  $\omega t$  between  $-\pi$  and  $\pi$ .